The Effect of Surface Albedo Heterogeneity on Sky Radiance

P. J. Ricchiazzi
Institute for Computation Earth System Science
University of California at Santa Barbara
Santa Barbara, California

A. Payton
Department of Geography
University of California at Santa Barbara
Santa Barbara, California

C. Gautier
Institute for Computation Earth System Science and Department of Geography
University of California at Santa Barbara
Santa Barbara, California

Abstract

The sky radiance at a high-latitude, coastal site was measured under clear and cloudy conditions with an all-sky camera and a narrow field-of-view spectroradiometer. The observations were compared to computational results from a three-dimensional (3-D) Monte-Carlo radiation model that explicitly includes the interaction of radiation with heterogeneous surface features. The sky radiance distribution roughly mirrors the spatial distribution of surface albedo, and shows good agreement with modeled results.

Introduction

Downwelling radiation over a highly reflecting surface is increased by multiple reflection between the surface and sky, especially when clouds are present. Several previous studies documented this effect in regions of uniform surface reflectivity (Leontyeva and Stamnes 1994; Gardiner, 1987). However, less is known about the level of increase expected near an abrupt transition in surface albedo, such as found at a high-latitude coastal site free of ocean ice. This information is required to understand surface radiation measurements at such locations.

Since about 1987, the Antarctic Monitoring System, sponsored by the National Science Foundation, has been gathering high-resolution ultraviolet (UV) radiation spectra from three sites in Antarctica: South Pole, McMurdo, and Palmer Stations. The observations from Palmer Station are of special interest because of its proximity to a highly productive marine ecology that may be stressed by the enhanced levels of UV radiation that occur in the austral spring. UV observations from Palmer provide

the best long-term dataset with which to assess how ozone depletion affects bio-productivity of the Southern Ocean. It is important to quantify how non-homogeneous surface reflectance impacts the interpretation of this data.

In this study, we will present observations of sky radiance obtained at Palmer Station with an all-sky camera and an Analog Spectral Devices spectroradiometer. The measured radiance values for several cloudy and one clear-sky day will be compared to results from a 3-D Monte-Carlo radiation model that explicitly includes the interaction of radiation with heterogeneous surface features (Ricchiazzi and Gautier 1998).

Observations

Sky radiance was measured with a FieldSpec radiometer manufactured by Analytical Spectral Devices (ASD). The ASD was configured with a one-degree foreoptic and recorded radiance data at one nanometer resolution between 350 nm and 2500 nm. Observations were made at about 3 pm local time over several cloudy days and one clear-sky day. Scans of the sky radiance were made in a vertical plane perpendicular to the solar principle plane, from the northeast to the southwest, with stops at 15-degree intervals. This scanning direction is roughly aligned along the major gradient of the surface albedo with the glacier to the northeast and the ocean to the southwest.

The multi-filter rotating shadowband radiometer (MFRSR) was used as a cross-calibration reference for the ASD radiance. The MFRSR measures the total, diffuse, and direct components of solar irradiance at six discrete channels between 300 nm and 1000 nm. The MFRSR recorded data at 1-minute time intervals. The total irradiance values in the first five channels are used here. The ASD scans were performed directly adjacent to the MFRSR station.

Global views of sky brightness were obtained before and after the ASD radiance observations with a Nikon 950 digital camera fitted with a fisheye lens. In addition, to verify that the ocean area was indeed free of ice, aerial photographs of the surface were obtained using the digital camera attached to a tethered helium balloon. Figure 1 shows a view from the balloon, at 500 m altitude, taken on November 27, 1999. The image shows the edge of Piedmont Glacier, Arthur Harbor, and the ocean area several tens of kilometers around the station. The station itself is located at the bottom-center of the image, where exposed rock is visible. Previous modeling results indicate that the radiation environment in the vicinity of the station may be affected by surface features up to 5 km away (Ricchiazzi and Gautier 1998).

Data Processing

ASD radiance was measured for a white reference (Spectralon) before and after each set of nine angular scans. The white reference scans were corrected for the known wavelength dependence of Spectralon. Since Spectralon very closely approximates a Lambertian reflector, the ASD white reference scans can be interpreted as an irradiance and directly related to the MFRSR data. The ratio of the concurrent MFRSR measurement and the ASD white reference scans provides a calibration factor at the beginning

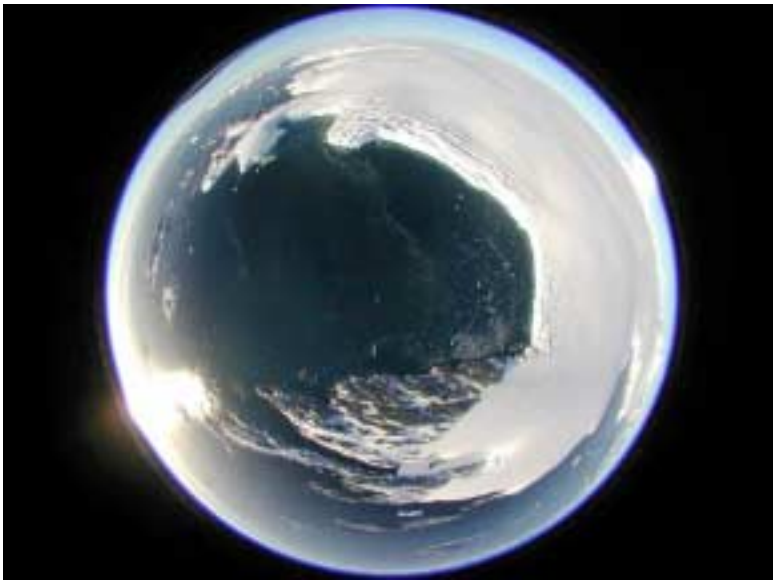

Figure 1. Balloon image for November 27, 1999. Surface conditions (ocean and glacier) remained fairly constant between November 20, 1999, and December 1, 1999.

and end of a series of angular scans. The calibration factor appropriate to a given zenith angle was obtained by time interpolation. This calibration procedure was used to eliminate the effects of gain instability in the ASD spectrometer.

Calculations

Sky radiance was computed with a Monte Carlo radiative transfer code (Ricchiazzi and Gautier 1998). The calculations treat a 3-D atmospheric volume, which extends from the surface to 100 km altitude, and has a 20 km x 20 km footprint centered on Palmer Station. The radiative transfer calculations include the effects of molecular absorption, cloud scattering, and reflection by ocean and snow. The accuracy of the Monte Carlo code was evaluated by comparison with a plane-parallel radiative transfer model (Ricchiazzi et al. 1998) for a one-dimension case with zero surface reflectance. As shown in Figure 2, the Monte Carlo results closely match the shape and magnitude of the radiance distribution computed by the plane-parallel model. In the full 3-D calculations, surface reflection is modeled explicitly, taking into account the island's surface topography and snow bidirection reflectance distribution function (BRDF). To expedite the calculations, radiance was computed by reverse propagation. A photon source at Palmer Station was scanned through a discrete set of viewing directions (an array of nine azimuths and six zenith angles), and the statistics for 30,000 photons in each viewing direction was accumulated. Calculations were performed at the MFRSR wavelengths (414, 500, 609, 665, and 861 nm), and for cloud optical depths of 15 and 30.

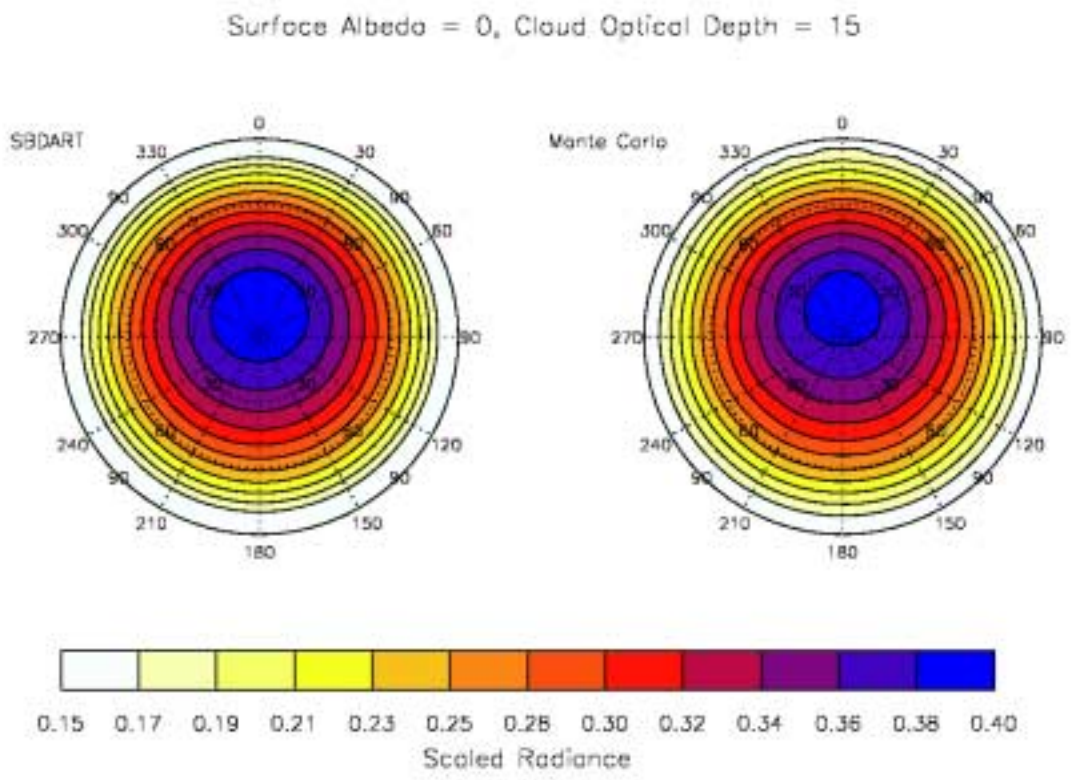

Figure 2. Comparison of Monte Carlo radiance computation with a plane-parallel radiative transfer model (SBDART) assuming zero surface reflectance.

Discussion

Figure 3 shows the normalized radiance (radiance divided by zenith radiance) predicted by the model for the 414-nm and 861-nm channels, and for cloud optical depth 15 and 30. The model computations predict that the level of sky radiance enhancement over the glacier is wavelength-dependent due to the spectral variation of snow reflectivity. For the optical depth 30 case, the enhancement is about 30% for the 414-nm channel, but only 20% for the 861-nm channel. In the sea-ward direction, the normalized radiance is essentially the same for the two channels.

Figure 4 shows the all-sky image for November 20, 1999. The ASD spectral observations for that day are shown in Figure 5. The sky radiance increases for all wavelengths as the viewing angle is scanned from the SW through the zenith and to the NE (except for the strong absorption in the Oxygen A band). The lower plot in Figure 5 shows a comparison of the observed normalized radiance with the Monte Carlo results. The computed radiance for thin (diamonds) and thick (triangles) clouds brackets the observations for each viewing direction. In addition, the downward trend with wavelength of the 60NE (toward glacier) scan seems to be well reproduced in the simulation.

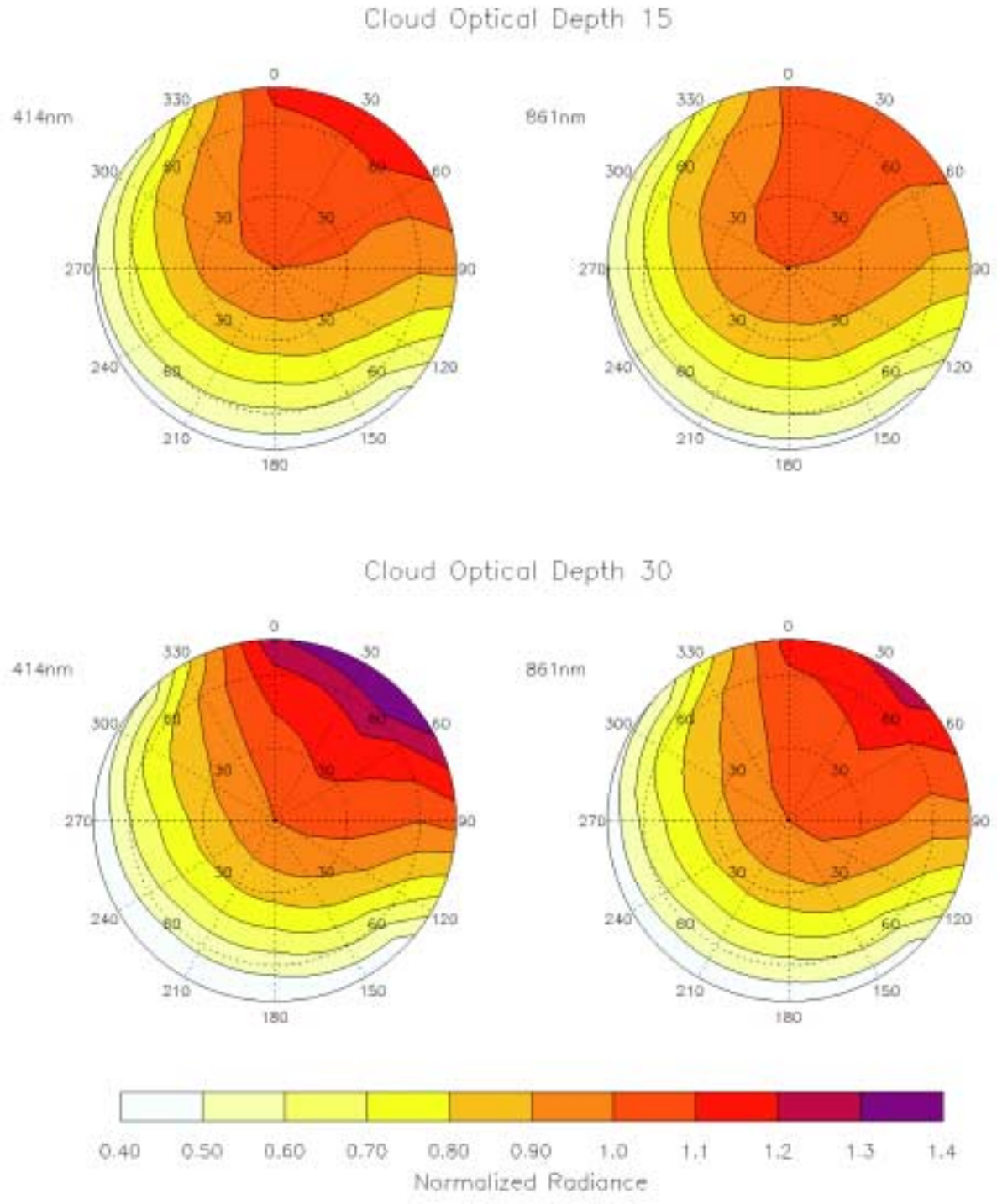

Figure 3. Computed 3-D radiance distribution for the 414-nm and 861-nm channels, for cloud optical depth 15 and 30. The glacier is to the NE.

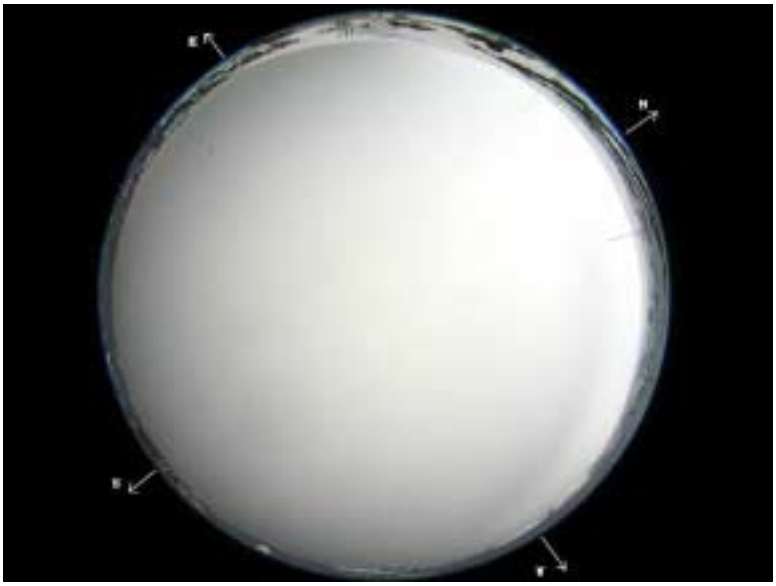

Figure 4. All sky image for November 20, 1999.

Overall, the results for December 1, 1999 (Figures 6 and 7), do not agree as well. Though the match is fairly good in the SW direction, the normalized radiance is much greater than the model predictions in the NE direction. Furthermore, the constancy of the normalized radiance with wavelength over the glacier (60NE) is inconsistent with the model calculations. For the conditions on this day, it appears that multiple reflection between the cloud and glacier does not decrease radiance levels toward the red and near-IR as it does for the November 20, 1999, case. This may be due the nature of the cloud layer, which, according to the all-sky image, has much greater horizontal structure than for November 20, 1999.

Summary

Comparisons of 3-D calculations of sky brightness with observations on two cloudy days indicate fairly good agreement when the cloud field is free of horizontal structure. In the case where the strataform layer did have horizontal structure, brightening over the snow-covered area was observed, but details of the sky radiance spectral profile did not agree with model simulations. Clearly, a much greater number of observations are required to understand the effects of albedo transition at the coast. In addition, model calculations in the spectral region near the Oxygen A band may reveal more information about how the surface/cloud interactions affect the sky radiance.

Corresponding Author

P. J. Ricchiazzi, paul@icess.ucsb.edu, (805) 893-4310

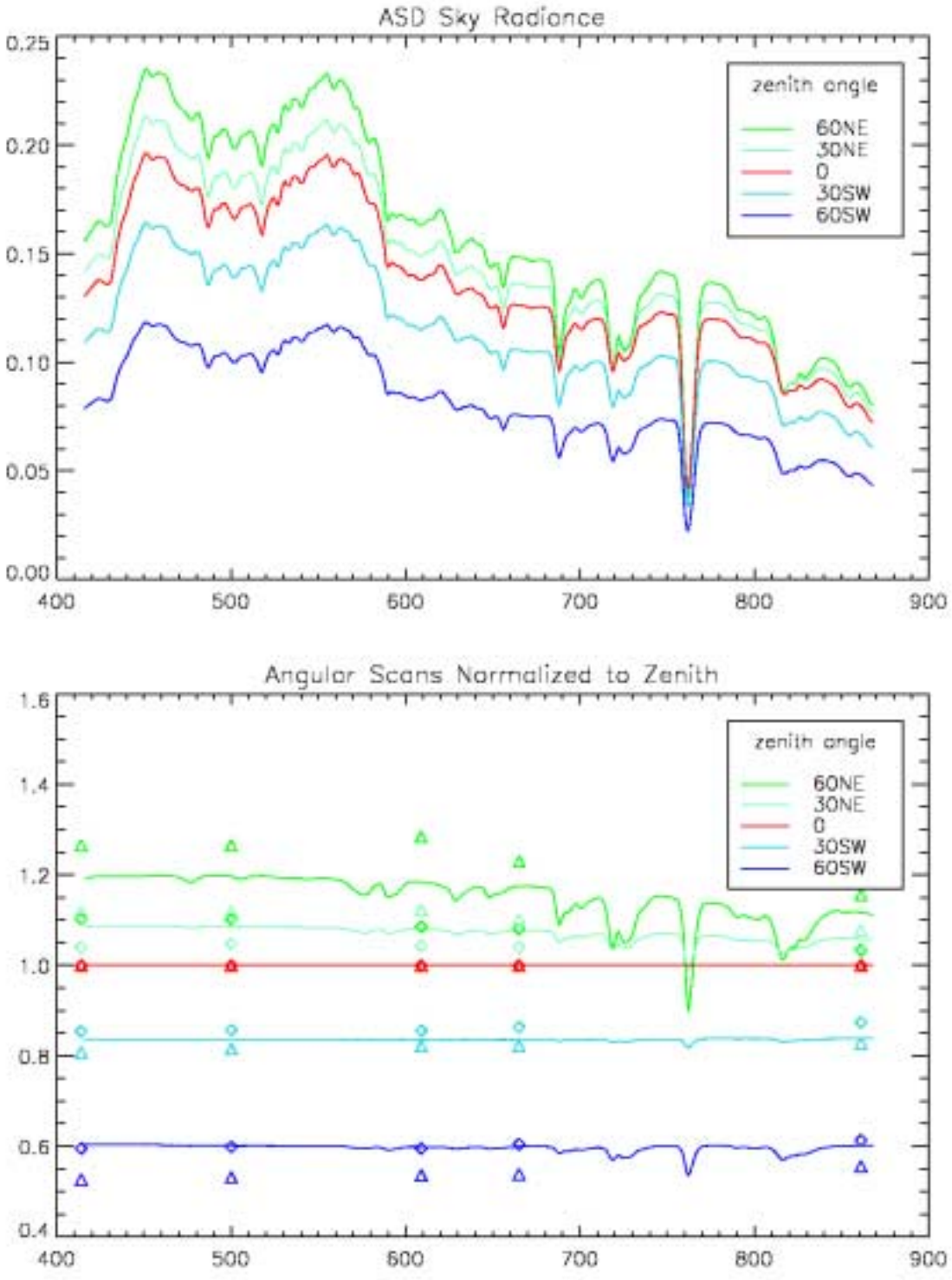

Figure 5. ASD radiance scan for November 20, 1999 (upper). Radiance at each viewing angle normalized to the zenith radiance is shown in the lower panel. Computer results are shown as diamonds ($\tau = 15$) and triangles ($\tau = 30$).

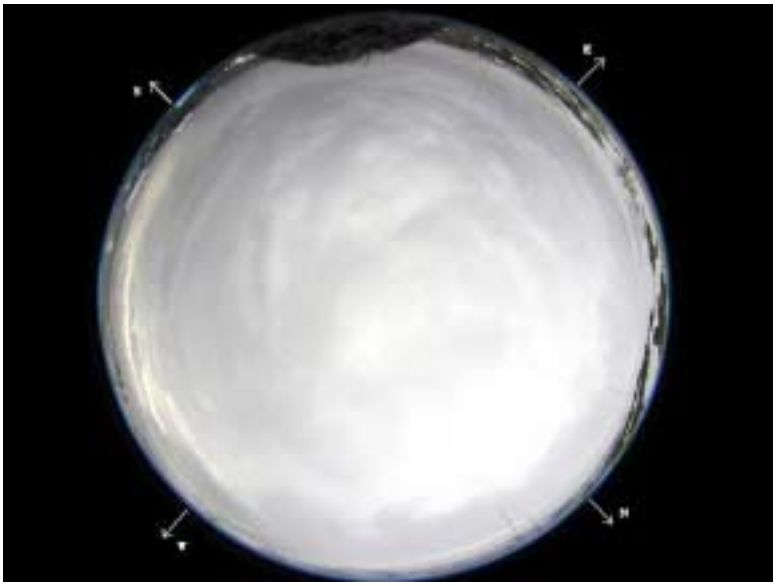

Figure 6. Same as Figure 4 for December 1, 1999.

References

Gardiner, B. G., 1987: Solar radiation transmitted to ground through cloud in r elation to surface albedo. *J. Geophys. Res.*, **92**, 4010-4018.

Leontyeva, E., and K. Stamnes, 1994: Estimations of cloud optical thickness from ground-based measurements of incoming solar radiation in the arctic. *J. Climate*, **7**(4), 566-578.

Ricchiazzi, P., and C. Gautier, 1998: Investigation of the effect of surface heterogeneity and topography on the radiation environment of Palmer Station, Antarctica, with a hybrid 3-D radiative transfer model. *J. Geophys. Res.-Atmos.*, **103**(D6), 6161-6176.

Ricchiazzi, P., S. R. Yang, and C. Gautier, 1998: SBDART: A research and teaching software tool for plane-parallel radiative transfer in the Earth's atmosphere. *Bull. Amer. Met. Soc*., **79**(10), 2101-2114.

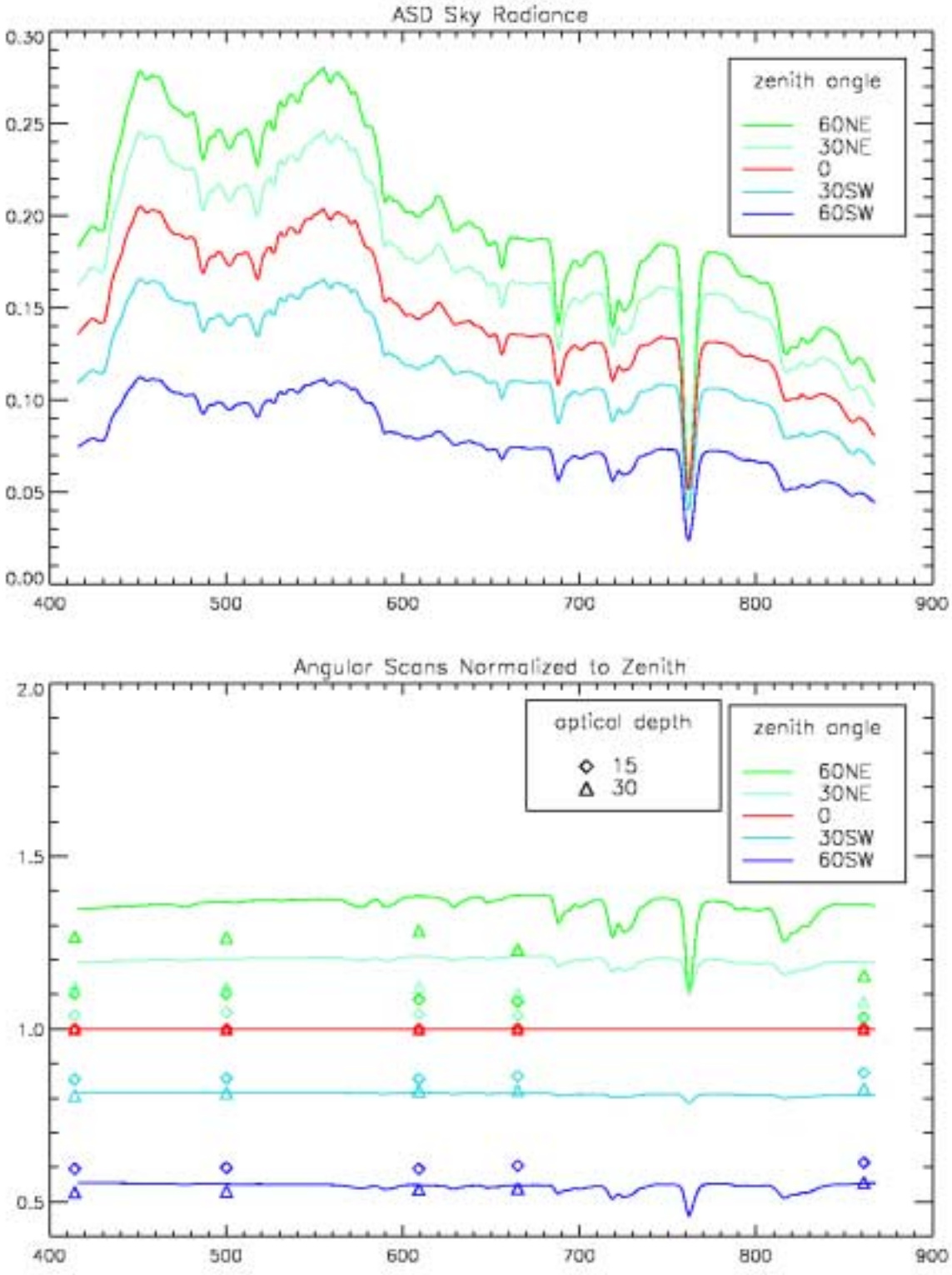

Figure 7. Same as Figure 5 except for December 1, 1999.